Scripta Materialia 131 (2017) 59–62

Contents lists available at ScienceDirect

Scripta Materialia

journal homepage: www.elsevier.com/locate/scriptamat

Regular Article

On the elusive crystal structure of expanded austenite

Bastian K. Brink [a,c], Kenny Ståhl [b], Thomas L. Christiansen [a], Jette Oddershede [c], Grethe Winther [a], Marcel A.J. Somers [a,*]

[a] Department of Mechanical Engineering, Technical University of Denmark, Produktionstorvet B425, DK-2800 Kgs. Lyngby, Denmark
[b] Department of Chemistry, Technical University of Denmark, Kemitorvet B206, DK-2800 Kgs. Lyngby, Denmark
[c] Department of Physics, Technical University of Denmark, Fysikvej B307, DK-2800 Kgs. Lyngby, Denmark

ARTICLE INFO

Article history:
Received 24 November 2016
Received in revised form 2 January 2017
Accepted 5 January 2017
Available online xxxx

Keywords:
Expanded austenite
Crystal structure
Plastic deformation
Nitriding
X-ray diffraction (XRD)

ABSTRACT

No consistent structural description exists for expanded austenite that accurately accounts for the *hkl*-dependent peak shifts and broadening observed in diffraction experiments. The best available description for homogeneous samples is a face-centered cubic lattice with stacking faults. Here Debye simulations of stacking fault effects were compared to experimental data for macro-stress free homogeneous expanded austenite to show that a faulted structure cannot explain the observed peak displacement anomalies. Instead it is argued that the shifts are the combined result of elastic and plastic anisotropy leading to (strongly) non-linear *hkl*-dependent elastic behavior during composition-induced plastic deformation on synthesis of expanded austenite.

Low temperature surface treatment of austenitic stainless steel, by dissolving nitrogen and/or carbon into the supersaturated solid solution in the austenite lattice, leads to the development of a surface-adjacent zone of so-called expanded austenite. Despite more than three decades of research on expanded austenite [1–3], there is currently no consistent structural description that accurately accounts for the *hkl*-dependent shifts and broadening observed in diffraction experiments. The most prominent complicating feature of diffractograms of, most notably, nitrogen-stabilized expanded austenite, are the anomalous positions of the 200 (and to a lesser degree 311) reflection(s), which are shifted to lower diffraction angles as compared to an ideal f.c.c. (face-centered cubic) lattice [4] (cf. the upper part of Fig. 1). In addition anisotropic broadening is observed, which is least pronounced for the 111 reflection. The best available description for the anomalous shift of the 200 reflection of an expanded austenite zone grown into an austenitic stainless steel, first proposed by Sun et al. [4], is the effect of elastic anisotropy in the strained expanded austenite surface zone and an enhanced stacking fault density. The presence of stacking faults in expanded austenite has been observed directly with transmission electron microscopy [5,6]. The applicability of Sun et al.'s interpretation was convincingly demonstrated for the 111, 200 and 220 peaks of macro-stress free homogeneously nitrided samples of uniform composition, where only the effect of stacking faults needs to be considered [7,8], using Warren's [9] theory to account for the systematic shifts by the presence of stacking faults. For such homogenous samples relatively low stacking fault probabilities were sufficient to explain the relative shifts of the investigated *hkl*.

Apart from the few investigations on homogeneous (gradient free) samples, all other investigations in the literature rely on heterogeneous samples with both a composition profile and a macro-stress profile in the depth direction. Fewell & Priest [10] reviewed ten plausible candidate structures on the basis of synchrotron X-ray diffraction on an expanded austenite zone grown into an austenite substrate. The outcome of their systematic investigation was that no simple structural model is sufficient to describe expanded austenite, and that most likely a combination of elastic anisotropy and faulting is responsible for the observed diffraction patterns of their (strained) sample, i.e. consistent with the original suggestion by Sun et al. [4]. The individual contributions of *hkl*-dependent lattice strain and stacking fault density to peak shifts have previously been demonstrated for simulated X-ray diffractograms [11].

Concerning the prediction of the *hkl*-dependent peak shifts due to stacking faults, it has been demonstrated that Warren's approach is insufficiently accurate due to unrealistic simplifying assumptions [12]. In Warren's analysis [9] the various profile components comprising a diffraction peak are not equally affected, or may be largely unaffected by stacking faults. Velterop et al. [12] showed convincingly that a weighted summation should be used, but unfortunately, their approach is too complicated to be readily implemented in a Rietveld procedure. Recently, in an effort to obtain a simple (approximate) relation between stacking fault probability, peak shift and peak broadening, avoiding the simplifying assumptions of Warren, Debye simulations of X-ray diffractograms were adopted to verify whether the stacking fault

* Corresponding author.
E-mail address: somers@mek.dtu.dk (M.A.J. Somers).

http://dx.doi.org/10.1016/j.scriptamat.2017.01.006
1359-6462/

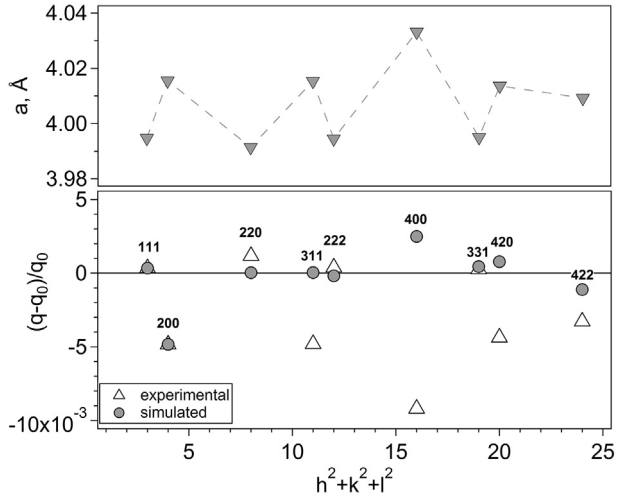

Fig. 1. Apparent lattice parameter, *a*, determined from experimental peak positions (upper part) and comparison to simulated peak shifts, expressed as the relative difference in magnitude of the scattering vector *q*, caused by intrinsic stacking faults according to Debye simulations [13] fitted to match the 111 and 200 peak of experimental data for nitrogen expanded austenite [28] (lower part).

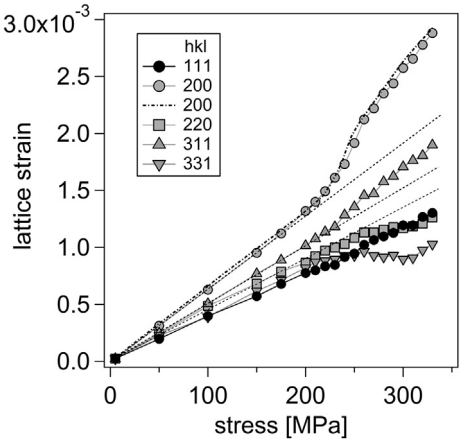

Fig. 2. Experimental lattice strains for selected *hkl* as measured with neutron diffraction in the direction parallel to the uniaxial tensile stress applied onto stainless steel. For comparison the predicted lattice strain for 200 is included and represented by the dash-dot line (all experimental data and simulations from [20]). The thin dashed straight lines extrapolate the elastic regime for 200, 220 and 311 reflections to emphasize the non-linearities introduced by plastic deformation.

model provides an accurate interpretation of the peak shifts for *hkl* beyond 220 [13]. The main results of these simulations are provided below.

An aspect of the expanded austenite zone that hitherto has not been included in the interpretation of *hkl*-dependent shifts is the occurrence of strong plastic deformation of the lattice as a consequence of a plastic accommodation of the composition-induced volume expansion. Several experimental investigations of the microstructure of expanded austenite [8,14–16] as well as modelling of composition and stress profiles [17], have demonstrated that the composition-induced lattice expansion in expanded austenite is largely accommodated by substantial plastic deformation, which develops under a state of (rotationally symmetric) biaxial stress within the plane of the expanded austenite zone. The plastic strain in the direction perpendicular to the surface was calculated to be as high as 16% [18]. Austenitic stainless steel is strongly elastically anisotropic with an elastically compliant ⟨100⟩ direction while the ⟨111⟩ direction is rigid. Adopting a self-consistent model by Hutchinson [19], Clausen et al. [20] investigated the *hkl* specific lattice strains parallel to and perpendicular to the load axis for uniaxial tension of f.c.c. polycrystals (Al, Cu and stainless steel) in the plastic region. In this respect it is important to realize that, from a mechanical point of view, the rotationally symmetric biaxial state of compressive stress in expanded austenite deviates by only a hydrostatic stress component from a uniaxial tensile load in the direction perpendicular to the surface. Consequently, provided that free-surface effects can be neglected, the lattice strain and plasticity in expanded austenite in the direction perpendicular to the surface is equivalent to that parallel to a uniaxial tensile direction, as was demonstrated to apply for the lattice rotations in expanded austenite grains [21]. Results similar to those reported by Clausen et al. were obtained with a three dimensional crystal plasticity-based finite element model [22]. The simulated *hkl*-dependent response was corroborated by in-situ neutron diffraction lattice strain determination [20,23]. The results obtained with simulation and in-situ neutron diffraction show a high degree of non-linear behavior in the plastic regime, in particular for the 200 lattice strains (Fig. 2). As will be discussed these results shed a new light on the anomalies observed in X-ray diffractograms of expanded austenite.

Recently, it was reported on the basis of investigations with nano-indentation [24,25] that the anisotropy of expanded austenite appears to be reversed as compared to the elastic anisotropy of stainless steel. Moreover, comparison of X-ray diffraction lattice strains probed on 111 and 200 reflections suggested that the ratio of the elastic constants of the crystallographic directions ⟨111⟩ and ⟨200⟩ changes with nitrogen content [26]. Also these results could be a consequence of the non-linear behavior of (expanded) austenite in the plastic regime.

The diffracted intensity of randomly oriented identical scattering objects can be calculated as a sum over all the interatomic distances according to the Debye scattering equation [27]. Accordingly, it is possible to calculate the diffracted intensity of any atomic array defined in terms of crystallographic parameters such as atomic composition, coordinates and thermal parameters and explore the effects of crystallographic defects like stacking faults. For the current simulations a modified version of the Debye program developed by Oddershede et al. [28] was applied. All details of the calculations, which yielded shifts consistent with those of Velterop et al. [12], were given in [13].

Simulated peak shifts are compared to synchrotron X-ray diffraction data previously obtained [28] for a homogeneous sample of nitrogen expanded austenite with interstitial occupancy (i.e. the number nitrogen atoms per metal atom), $y_N = 0.61$, with reported lattice parameter, $a = 4.0022$ Å and stacking fault probability, $\alpha_{sf} = 0.0362$ (according to Warren's method) in Fig. 1 (lower part). Here q_0 refers to the unfaulted position and q to the shifted position where $q = 4\pi\sin\theta/\lambda$ is the magnitude of the scattering vector. Since q_0 is not known, a combination of lattice parameter, *a*, and intrinsic stacking fault probability was optimized to match the experimental 111 and 200 peak positions for nitrogen expanded austenite (giving $a = 3.9961$ Å and $\alpha_{sf} = 0.06$). If the stacking fault model would apply, the peak shifts of higher *hkl* should align reasonably with the predicted values. Evidently, comparing experimental and simulated peak shifts in Fig.1 such a correspondence may be obtained for 220, 222 and 331, while major discrepancies occur for 311, 400, 420 and (to a lesser extent) 422. Fig. 1 illustrates that deceptively reasonable fits can be obtained when only the first three reflections, i.e. 111, 200 and 220 are considered (even for the Warren model), as in previous investigations [7,8]. If only these reflections are available, as is the case on applying Cr K_α radiation, the intuitive conclusion is that the systematic peak shifts can actually be explained from the presence of stacking faults in the f.c.c. lattice. The current analysis demonstrates that stacking faults alone cannot consistently explain the systematic shifts of the reflections of a macro-stress free homogeneous sample of expanded austenite.

As was demonstrated by self-consistent [20] and finite element [22] crystal plasticity modelling and verified by neutron diffraction data [20, 23], the relation between the applied tensile stress and the elastic strain for certain reflections in the elasto-plastic regime is highly non-linear (see Fig. 2). The on-set of non-linearity at the elasto-plastic transition